A Novel Fuel Performance Index for Low-Temperature Combustion Engines Based on Operating Envelopes in Light-Duty Driving Cycle Simulations

A Novel Fuel Performance Index For LTC Engines Based On Operating Envelopes In Light-Duty Driving Cycle Simulations

Kyle E. Niemeyer*

School of Mechanical, Industrial,

and Manufacturing Engineering

Oregon State University

Corvallis, Oregon, 97330

Email: Kyle.Niemeyer@oregonstate.edu

Shane R. Daly

School of Mechanical, Industrial,

and Manufacturing Engineering

Oregon State University

Corvallis, Oregon, 97330

Email: dalys@onid.oregonstate.edu

William J. Cannella

Chevron Energy Technology Company

Richmond, California, 94802

Email: bijc@chevron.com

Christopher L. Hagen

School of Mechanical, Industrial,

and Manufacturing Engineering

Oregon State University

Bend, Oregon, 97701

Email: Chris.Hagen@oregonstate.edu

ABSTRACT

Low-temperature combustion (LTC) engine concepts such as homogeneous charge compression ignition (HCCI) offer the potential of improved efficiency and reduced emissions of NO_x and particulates. However, engines can only successfully operate in HCCI mode for limited operating ranges that vary depending on the fuel composition. Unfortunately, traditional ratings such as octane number poorly predict the autoignition behavior of fuels in such engine modes, and metrics recently proposed for HCCI engines have areas of improvement when wide ranges of fuels are considered. In this study, a new index for ranking fuel suitability for LTC engines was defined, based on the fraction of potential fuel savings achieved in the FTP-75 light-duty vehicle driving cycle. Driving cycle simulations were performed using a typical light-duty passenger vehicle, providing pairs of engine speed and load points. Separately, single-zone naturally aspirated HCCI engine simulations were performed for a variety of fuels in order to determine the operating envelopes for each. These results were combined to determine the varying improvement in fuel economy offered by fuels, forming the basis for a fuel performance index. Results showed that, in general, lower octane fuels performed better, resulting in higher LTC fuel index values; however, octane number alone did not predict fuel performance.

1 Introduction

Due to federal directives to improve fuel economy and reduce pollutant emissions, significant research efforts are currently focused on advanced combustion strategies for internal combustion engines. Many of these strategies focus on the low temperature combustion (LTC) regime, such as homogeneous charge compression ignition (HCCI), which combines beneficial aspects of spark-ignition (SI) and compression-ignition (CI) engines to offer the best of both worlds. HCCI engines can operate unthrottled at high compression ratios and with a lean fuel-air mixture, which results in lower combustion temperatures than conventional engines, together leading to improved thermal efficiency over SI engines and significantly reduced NO_x production. Similar to CI engines, HCCI engines control the load by varying the amount of fuel mixed with air, avoiding the major pumping losses associated with throttling in SI engines. However, unlike CI engines, the fuel and air are premixed, resulting in low particulate emissions [1, 2].

While HCCI engines have received significant research attention since first introduced [3, 4]—and continue to receive attention, albeit alongside related concepts such as reactivity controlled compression ignition (RCCI) [5–8], which varies fuel reactivity by stratifying a lower reactivity fuel like gasoline with a highly reactive fuel like diesel—a number of research challenges remain. Unlike SI and CI engines, where the spark and fuel injection initiate combustion, respectively, complex autoignition chemistry controls the combustion timing in HCCI and other LTC engines. As a result, various fuels offer different, limited operating ranges in HCCI engines. In addition, while HCCI combustion results in reduced nitrogen oxide (NO_x) emissions due to lower temperatures, high levels of carbon monoxide and unburned hydrocarbons remain [2]. Yao et al. [2] reviewed additional challenges in HCCI engine research, and various strategies developed to tackle them.

Early studies on HCCI strategies with gasoline [3, 4, 9] found that successful HCCI combustion could only be achieved

*Address all correspondence to this author.

in limited operating ranges. With a typical SI compression ratio, the resistance to knock of typical high-octane gasoline prevents the initiation of autoignition at low loads and idle. At higher loads, knocking occurs. Diesel fuel, on the other hand, is much more reactive than gasoline, and ignites early (knocks) when used in a premixed charge at the high compression ratios typical of CI engines [1]. While strategies to use typical gasoline and diesel fuels in HCCI engines have been investigated [1, 2], another option is to find new fuels, or fuel blends, that may offer more attractive performance. Various groups have investigated in this direction, studying the operating ranges of different fuels in HCCI engines [10–22]. However, despite this research activity, a robust method to rank fuel performance—as well as predict it—in HCCI and other LTC-strategy engines has not yet emerged.

1.1 Need for a new index

The octane number (ON)—the average of the research octane number (RON) and motor octane number (MON)—is used to rank a gasoline fuel's resistance to knock, where a higher number indicates greater knock resistance. These values are determined by comparing the knocking characteristics under standardized conditions to those of a binary mixture of n-heptane and 2,2,4-trimethylpentane (iso-octane), where 0 and 100 correspond to neat n-heptane and iso-octane, respectively. These two fuels make up the so-called primary reference fuels (PRFs). However, because real fuels consist of more complex mixtures of fuel components compared to the PRFs, various studies showed that octane rating does not adequately predict autoignition in HCCI engines [14, 15, 22].

In order to better quantify fuel performance in HCCI engines, a number of new metrics have been proposed. Kalghatgi [14] introduced the octane index (OI), which includes information about engine-specific operating conditions along with the RON and MON values. Shibata and Urushihara [15] developed three HCCI fuel indices, including the relative HCCI index that combines MON with information about the fuel components: the volume percentage of n-paraffins, iso-paraffins, olefins, aromatics, and oxygenates. However, as Rapp et al. [22] recently showed in a study of the performance of various fuels in a Cooperative Fuel Research (CFR) engine operating in HCCI mode, neither octane nor relative HCCI index could predict the autoignition behavior of many fuels, in particular gasoline blends including naphthenes, aromatics, and ethanol.

Therefore, a new metric for measuring the performance of fuels in LTC engines needs to be developed, in order to both rank fuels and predict future performance. Such a metric could be used to identify attractive fuels for HCCI engine operation, or assist in the development of new fuels. In the current work, a new LTC fuel index is introduced that seeks to combine information about the operating envelope—the feasible engine speeds and loads for the fuel in HCCI mode—while focusing on practical conditions (i.e., operating points useful for realistic driving conditions). In other words, fuels with wide operating ranges that are outside the conditions needed for typical vehicles in typical driving conditions should not be highly ranked because the actual impact on fuel consumption would be minimal. We will do this by simulating transient driving cycles to obtain required engine operating loads and baseline fuel consumption, in order to gauge the impact of various fuels on the vehicle fuel economy.

While significant research activity has focused on studying advanced IC engine development, including HCCI and related concepts, only a handful of studies used transient driving cycles to predict fuel economy and emissions improvements

using these advanced engine modes. Zhao et al. [23] simulated a hybrid SI/HCCI gasoline engine through the European New Emission Drive Cycle, reporting only moderate improvements in fuel economy and emissions due to a limited HCCI range over the conditions experienced in the driving cycle. Curran et al. [24] approximated the EPA Federal Test Procedure (FTP-75) driving cycle using five steady-state modal points [25, 26] and compared fuel economy and emissions of RCCI, diesel HCCI, and conventional diesel combustion. Gao et al. [27, 28] performed simulations of light-duty conventional and hybrid-electric vehicles equipped with HCCI-capable diesel engines over the Urban Dynamic Driving Schedule (UDDS), finding that the conventional vehicle benefited from HCCI operation in terms of fuel consumption and emissions. However, since the hybrid-electric vehicle only needed the diesel engine for higher loads, HCCI offered little improvement due to its limited operation range. Ortiz-Soto et al. [29] developed an engine and vehicle modeling framework that they used to simulate a hybrid SI/HCCI engine-powered vehicle over the EPA UDDS, Highway Fuel Economy Test, and US06 driving cycles. Ahn et al. [30] later used this methodology to model vehicles with hybrid-electric engines capable of dual SI/HCCI operation, finding results consistent with those of Gao et al. [27, 28] mentioned above. However, none of these studies explored the performance of various fuels over the driving cycles, or sought to find a new fuels that might offer wider HCCI operating envelopes.

In the current study, we performed driving cycle simulations for a typical light-duty passenger vehicle, generating steady-state operating points in terms of engine speed and torque, and also obtained the corresponding baseline SI engine fuel consumption for these operating points. Next, HCCI engine simulations were performed for a variety of fuels in order to determine their operating ranges. The resulting operating envelopes were combined with the necessary operating points for the driving cycle, and we defined new fuel index based on the potential fuel savings achieved by switching to HCCI combustion for the feasible points.

2 Methodology

2.1 Driving cycle simulation

In order to determine desirable fuel operating ranges for HCCI combustion, we performed simulations of a light-duty passenger vehicle in the US EPA FTP-75 driving cycle [31]. Figure 1 shows the specified vehicle speed as a function of time for this driving cycle. This driving cycle attempts to emulate typical urban driving conditions with a short cold start phase, a transient phase, and a hot start phase; it is used to measure the fuel economy and emissions of passenger cars in the United States. It covers a total distance of 17.8 km in 1874 s (not including the 10 min break observed in Fig. 1), with an average vehicle speed of 34.1 $\mathrm{km\,h^{-1}}$.

We chose the Toyota Camry—the best-selling passenger car in North America in recent years—for the modeled vehicle as a representative of typical light-duty vehicles in North America. In order to simulate the performance—and the fuel consumption in particular—of this vehicle over the driving cycle, we used the ADvanced VehIcle SimulatOR (ADVISOR) [32, 33] package. ADVISOR is a hybrid backward/forward-facing vehicle simulator, meaning that it combines elements of backward-facing models, which start from the tractive force needed to move the vehicle at the directed speed, and forward-facing models, which start from a driver directing the engine to meet the necessary speed, to calculate fuel economy and

emissions of various vehicles over specified driving cycles. See Wipke et al. [32] or Gao et al. [34] for more detail on such models. ADVISOR interpolates data from experimental engine maps of steady-state fuel consumption rates and emissions, based on engine speed and torque, to model performance in the transient driving cycle.

We simulated the vehicle by modifying ADVISOR's default model for a small passenger car, VEH_SMCAR, which is based roughly on a 1994 Saturn SL1. The altered model, VEH_SMCAR_CAMRY, includes reference and estimated parameters for a 2012 Toyota Camry: coefficient of drag of 0.28, frontal area of 2.28 m^2, fraction of vehicle weight on front axle of 0.54, vehicle center-of-gravity height of 0.53 m, vehicle wheelbase of 2.775 m, and vehicle curb weight of 1447 kg. Coupled with this vehicle model, we used the FC_SI95 engine model, which is based on the Saturn 1.9 L dual overhead cam SI engine. This model includes maps of fuel use and emissions based on the experimental data of Reilly et al. [35]. We scaled the model engine from the default maximum power of 95 kW to 133 kW, to more closely match the Camry's engine.

Driving cycle calculations performed by ADVISOR return pairs of engine speed and torque in one second intervals. In order to compare these load requirements to the fuel operating envelopes described in the next section, we used the following basic relation for four-stroke engines to calculate the corresponding indicated mean effective pressure (imep) [36]:

$$\text{imep} = \frac{4\pi T}{V_d} , \tag{1}$$

where T indicates the torque and V_d the displacement volume.

2.2 Fuel operating envelope

In order to determine the fuel operating envelopes, we modeled an HCCI engine using the single-zone IC engine model of CHEMKIN version 10131 [37]. Rather than matching the engine of the Toyota Camry, we simulated the well-studied CFR engine, since numerous experimental results exist in the literature for this engine for comparison purposes. Furthermore, we avoided dependence of results on engine size by using imep instead of torque to compare engine performance between the driving cycle simulations and work output from the HCCI engine simulations (as will be described shortly). We emulated the CFR engine using the following geometry taken from Rapp et al. [22]: a cylinder displacement volume of 0.616 L, connecting rod to crank radius ratio of 4.44, and cylinder bore diameter of 82.8 mm. Simulations were performed from intake valve close to exhaust valve open, corresponding to 146° BTDC and 140° ATDC [11]. For the current study, we selected a compression ratio of 18.

Using the results from simulations that varied engine speed and fuel-air equivalence ratio, the upper limit for HCCI operation was defined at a maximum pressure rise rate ($dP/d\theta$) of 10 bar/(° CA) [11, 38]. We defined the lower limit as 90% molar conversion of C from fuel to CO_2, corresponding to incomplete combustion/misfire.

As in the previous section for torque, we converted the indicated work reported by CHEMKIN to imep, in order to readily

compare the calculated fuel operating envelopes to the engine operating points given for the driving cycle by ADVISOR:

$$\text{imep} = \frac{W_{c,i}}{V_d} , \tag{2}$$

where $W_{c,i}$ represents the indicated work per cycle.

2.3 LTC fuel index

By combining the results from the driving cycle simulations with the HCCI operating envelopes obtained for various fuels, we constructed a novel fuel index based on the potential fuel economy improvement offered by a fuel; it contains information about both the size and location of operating envelopes. Fuels with wide operating limits that also match ranges of operation important to real-world driving conditions will offer a greater real-world reduction in fuel consumption and therefore should be highly ranked. Due to a varying HCCI operation range, where SI operation will be required outside of the viable operating envelope, different fuels offer varying levels of fuel economy improvement.

The LTC fuel index is defined as the percentage of fuel savings achieved through HCCI operation; in other words, the fuel savings "actually" achieved divided by the potential fuel savings. First, we can calculate the potential fuel savings for full HCCI operation, $m_{fs,\text{HCCI}}$, based on the baseline SI fuel consumption over the entire driving cycle, $m_{f,\text{SI}}$:

$$m_{f,\text{HCCI}} = (1-\alpha) m_{f,\text{SI}} , \tag{3}$$

$$m_{fs,\text{HCCI}} = m_{f,\text{SI}} - (1-\alpha) m_{f,\text{SI}} , \tag{4}$$

$$= \alpha m_{f,\text{SI}} , \tag{5}$$

where α represents the potential improvement in fuel economy offered by HCCI over SI (e.g., 0.15–0.2 [1], 0.3 [23]) and $m_{f,\text{HCCI}}$ is the fuel consumption for full HCCI operation. The SI fuel consumption $m_{f,\text{SI}}$ is obtained from the ADVISOR driving cycle simulation, which reports the fuel consumption rate $\dot{m}_{f,\text{SI}}$ in one second intervals. Recognizing the limited operating range offered by HCCI, the fuel saved during hybrid SI/HCCI operation, $m_{fs,\text{SI+HCCI}}$, is given by

$$m_{fs,\text{SI+HCCI}} = m_{f,\text{SI}} - m_{f,\text{SI+HCCI}} , \tag{6}$$

$$= \alpha m_{f,\text{SI}\in\{\text{HCCI}\}} , \tag{7}$$

where $m_{f,\text{SI+HCCI}}$ is the fuel consumed over the hybrid SI/HCCI operation and $m_{f,\text{SI}\in\{\text{HCCI}\}}$ is the fuel consumed during the baseline SI operation over the possible HCCI operating range. In other words, the fuel saved during the hybrid SI/HCCI

operation is determined only by the fuel consumed during SI operation at the HCCI-viable operating points—the rest of the driving cycle is unaffected.

The fuel index is then defined as the percentage of fuel savings achieved:

$$I_{\text{HCCI}} = \frac{m_{fs,\text{SI+HCCI}}}{m_{fs,\text{HCCI}}} \cdot 100\% \,, \tag{8}$$

$$= \frac{\alpha m_{f,\text{SI}\in\{\text{HCCI}\}}}{\alpha m_{f,\text{SI}}} \cdot 100\% \,, \tag{9}$$

$$= \frac{m_{f,\text{SI}\in\{\text{HCCI}\}}}{m_{f,\text{SI}}} \cdot 100\% \,. \tag{10}$$

The index I_{HCCI} can also be interpreted as the mass-weighted percentage of discrete operating points for viable HCCI combustion. Therefore, the fuel index can be calculated independent of a specific HCCI fuel consumption improvement factor, although a constant improvement factor across the range of operating conditions is implicitly assumed.

2.4 Caveats and limitations

Note that since we performed the simulation over the compression and expansion strokes of the cycle, the gross indicated work per cycle was used. Furthermore, due to the idealized nature of these simulations, in the current work the calculated indicated work does not include friction losses. Therefore, the reported work and imep will be higher than the true values. Our approach is also unable to predict transient phenomena in the engine between the operating points, or switching from SI to HCCI operation. Gao et al. [39] developed a methodology to estimate transient effects from steady-state engine data, and used this to improve predictions of fuel consumption and emissions in vehicle driving cycle simulations. Nüesch et al. [40] also developed a model to predict transient effects from switching between the SI and HCCI combustion modes, finding that fuel consumption increased during transitions enough to nearly cancel out the HCCI improvements, and determined optimal timing delays to reduce these negative effects.

Finally, we note that the single-zone HCCI simulations used here assume spatial homogeneity, with no ability to capture spatial variations. In order to deal with this limitation, a number of engine modeling approaches have been developed that—while avoiding the cost of a spatially resolved, multidimensional computational fluid dynamics simulation—consider multiple zones to represent different regions within an engine (e.g., core, piston crevice, boundary layer) [41–45]. While these multi-zone models can more closely match experimental results, particularly for heat release rate, peak pressure, and unburned hydrocarbon emissions, the single-zone model adequately predicts the point of ignition as a function of inlet properties [44]. Furthermore, Yelvington et al. [12] showed that single-zone calculations could be used to accurately predict knock limits for HCCI combustion.

Noting these limitations, the current work is focused on demonstrating the methodology of constructing our fuel index, and showing some preliminary results. We are not comparing any computational results with experiments, but rather only comparing the calculations to each other in order to study trends and the relative performance of various fuels.

3 Results & discussion

First, ADVISOR was used to simulate the performance of the model Camry vehicle over the FTP-75 driving cycle. Figure 2 shows the resulting engine speed and torque operating points for the driving cycle. In addition, the fuel consumption rate in $\mathrm{g\,s^{-1}}$ is overlaid on the points. As expected, we observed higher fuel consumption rates at higher loads and engine speeds. Note that negative torque values occurred for this vehicle and driving cycle combination, corresponding to vehicle deceleration. While these points contributed to fuel economy due to nonzero fuel consumption rates—365 out of 2478 total operating points, or 12.4% of the total fuel consumption—our current HCCI engine model is not able to produce negative torque/imep values. Therefore, at best a fuel can currently achieve $I_{\mathrm{HCCI}} = 87.6$.

Next, we determined the fuel HCCI operating ranges for n-heptane and PRFs with 20, 40 and 70% iso-octane by molar percentage—fuels with octane numbers of 0, 21.7, 42.5 and 72.1, respectively—through CHEMKIN engine simulations. In order to search for operating points that corresponded to viable HCCI combustion over the specified driving cycle, these simulations were performed by varying equivalence ratio from 0.18 to 0.3 for all the fuels except PRF 40, which used the range 0.18 to 0.35, for engine speeds of 800 to 3000 rpm. We used the skeletal mechanism for PRFs of Tsurushima [46] developed for modeling HCCI combustion, which consists of 33 species and 38 reactions. We selected this compact mechanism over larger, more detailed reaction mechanisms (e.g., the PRF mechanism of Curran et al. [47, 48] with 1034 species and 1895 reactions) due to the large number of HCCI engine simulations performed; furthermore, the skeletal mechanism showed reasonable agreement with experimental results from shock tubes and HCCI engines [46]. Figure 3 shows the operating ranges in terms of equivalence ratio for these four fuels. Sample pressure profiles for each of the four fuels may be found in the Appendix. In general, lower octane PRFs (in particular n-heptane) demonstrated wider operating ranges in terms of both load and engine speed. Higher-octane PRFs had narrower but higher-load operating ranges, a trend consistent with literature experimental results for PRFs [11, 13, 38]. Interestingly, PRF 40 offered HCCI operation over the widest equivalence ratio range, which also translated to the widest load range.

Figure 4 shows the operating envelopes of the various PRFs, converted to imep, compared to the engine operating points for the driving cycle. First, note the relatively high imep values for the HCCI engine simulations; these resulted from the idealized nature of our engine simulations, neglecting friction losses that can account for 10–100% of the indicated work [36]. Accounting for frictional losses will reduce the calculated imep values, shifting downwards the operating envelopes for each fuel shown in Figs. 3 and 4. In the future, more realistic calculations will require an estimate for friction work using, e.g., an empirical correlation for total friction work based on engine speed [36], but these results serve the current objective of demonstrating the proposed fuel index and the methodology by which it is determined.

Finally, based on the results shown in Fig. 4, the LTC indices for the four fuels were calculated using Eq. (10) and are shown in Table 1. As expected based on the wide operating range shown in Figs. 3 and 4, n-heptane (ON = 0) has the highest index at 6.86. However, the index values did not monotonically decrease with increasing octane number; PRF 40 was ranked higher than PRF 20, due to operating envelope coverage over higher-fuel-consumption (i.e., higher load) points. This result further justifies the hypothesis that octane number is not a good predictor of fuel performance in HCCI engines.

While PRF 70 demonstrated viable HCCI operation—albeit in a fairly limited range of engine speeds—for the conditions

considered here, due to the operating envelope location no fuel savings over the driving cycle were achieved and therefore this fuel was assigned an index of zero. The ability of a fuel to support successful HCCI operation is necessary but not sufficient to improve fuel economy in realistic engine conditions—the operating envelope must cover practical engine speeds and loads.

4 Conclusions

In this work we developed a new metric to measure fuel performance in HCCI engines, based on the potential fuel economy improvement offered under realistic driving conditions. Different fuels offer varying ranges of HCCI operation, but a wide operating range alone does not guarantee real-world fuel savings—fuels with operating envelopes that cover practical engine speeds and loads should be favored. We obtained engine operating information by simulating the performance of a Toyota Camry, a popular passenger vehicle in North America, over the EPA FTP-75 (federal light-duty) transient driving cycle. Separately, we performed HCCI engine simulations for various fuels to determine the varying operation envelopes offered by each fuel. We then combined these data to create a fuel index measuring the percentage of fuel savings achieved, where 0 represents no fuel savings and 100 represents the full fuel savings achieved, corresponding to no viable HCCI operation and full HCCI combustion, respectively, over the driving cycle.

The operating envelopes for four PRF mixtures (0, 20, 40 and 70% iso-octane by molar percentage) were determined for a compression ratio of 18 and naturally aspirated intake conditions. Lower octane number corresponded to wider operating ranges, but higher octane PRFs could operate at higher equivalence ratios/engine loads. By combining the necessary driving cycle engine speeds and with the PRF operating envelopes, the LTC fuel index I_{HCCI} was calculated for each fuel. The lowest octane PRF considered (n-heptane) ranked highest using this metric, but the index value did not monotonically decrease with increasing octane number—consistent with literature results showing that octane number is not a sufficient metric for fuel performance in LTC engine modes. Our future work includes performing additional operating envelope and index calculations for fuel mixtures other than PRFs, including (but not limited to): toluene reference fuel blends (n-heptane, iso-octane, and toluene), methylcylcohexane, butane, butanol, ethanol, o-xylene, 2-pentene, and 1-hexene. In addition, we will explore the dependence of the fuel index on the particular driving cycle selected, including the New European Drive Cycle (NEDC) and Japanese JC08 tests.

Acknowledgements

The authors gratefully acknowledge the Chevron Energy Technology Company for supporting this research.

References

[1] Zhao, F., Asmus, T. W., Assanis, D. N., Dec, J. E., Eng, J. A., and Najt, P. M., 2003. *Homogeneous Charge Compression Ignition (HCCI) Engines: Key Research and Development Issues*. No. PT-94. SAE International, Warrendale, PA.

[2] Yao, M., Zheng, Z., and Liu, H., 2009. "Progress and recent trends in homogeneous charge compression ignition (HCCI) engines". *Prog. Energy Comb. Sci.,* ***35***(5), pp. 398–437.

[3] Onishi, S., Jo, S., Shoda, K., Jo, P., and Kato, S., 1979. Active thermo-atmosphere combustion (ATAC) – a new combustion process for internal combustion engines. SAE Technical Paper 790501.

[4] Najt, P. M., and Foster, D. E., 1983. Compression-ignited homogeneous charge combustion. SAE Technical Paper 830264.

[5] Kokjohn, S. L., Hanson, R. M., Splitter, D. A., and Reitz, R. D., 2010. "Experiments and modeling of dual-fuel HCCI and PCCI combustion using in-cylinder fuel blending". *SAE Int. J. Engines,* ***2***(2), pp. 24–39.

[6] Kokjohn, S. L., Hanson, R. M., Splitter, D. A., and Reitz, R. D., 2011. "Fuel reactivity controlled compression ignition (RCCI): a pathway to controlled high-efficiency clean combustion". *Int. J. Engine Res.,* ***12***(3), pp. 209–226.

[7] Curran, S. J., Hanson, R. M., and Wagner, R. M., 2012. "Reactivity controlled compression ignition combustion on a multi-cylinder light-duty diesel engine". *Int. J. Engine Res.,* ***13***(3), pp. 216–225.

[8] Splitter, D. A., and Reitz, R. D., 2013. "Fuel reactivity effects on the efficiency and operational window of dual-fuel compression ignition engines". *Fuel,* ***118***, pp. 163–175.

[9] Noguchi, M., Tanaka, Y., Tanaka, T., and Takeuchi, Y., 1979. A study on gasoline engine combustion by observation of intermediate reactive products during combustion. SAE Technical Paper 790840.

[10] Christensen, M., Hultqvist, A., and Johansson, B., 1999. Demonstrating the multi fuel capability of a homogeneous charge compression ignition engine with variable compression ratio. SAE Technical Paper 1999-01-3679.

[11] Aroonsrisopon, T., Sohm, V., Werner, P., Foster, D. E., Morikawa, T., and Iida, M., 2002. An investigation into the effect of fuel composition on HCCI combustion characteristics. SAE Technical Paper 2002-01-2830.

[12] Yelvington, P. E., Rallo, M. B. I., Liput, S., Tester, J. W., Green, W. H., and Yang, J., 2004. "Prediction of performance maps for homogeneous-charge compression-ignition engines". *Combust. Sci. Technol.,* ***176***(8), pp. 1243–1282.

[13] Atkins, M. J., and Koch, C. R., 2005. "The effect of fuel octane and dilutent on homogeneous charge compression ignition combustion". *Proc. IMechE. Part D: J. Automobile Engineering,* ***219***(5), pp. 665–675.

[14] Kalghatgi, G. T., 2005. Auto-ignition quality of practical fuels and implications for fuel requirements of future SI and HCCI engines. SAE Technical paper 2005-01-0239.

[15] Shibata, G., and Urushihara, T., 2007. Auto-ignition characteristics of hydrocarbons and development of HCCI fuel index. SAE Technical Paper 2007-01-0220.

[16] Ogura, T., Angelos, J. P., Green, W. H., Cheng, W. K., Kenney, T., and Xu, Y., 2008. Primary reference fuel behavior in a HCCI engine near the low-load limit. SAE Technical Paper 2008-01-1667.

[17] Liu, H., Yao, M., Zhang, B., and Zheng, Z., 2009. "Influence of fuel and operating conditions on combustion characteristics of a homogeneous charge compression ignition engine". *Energy Fuels,* ***23***, pp. 1422–1430.

[18] Starck, L., Lecointe, B., Forti, L., and Jeuland, N., 2010. "Impact of fuel characteristics on HCCI combustion: Performances and emissions". *Fuel,* ***89***(10), pp. 3069–3077.

[19] Aldawood, A. M., Mosbach, S., Kraft, M., and Amer, A. A., 2013. Dual-fuel effects on HCCI operating range:

Experiments with primary reference fuels. SAE Technical Paper 2013-01-1673.

[20] Han, X., Zheng, M., and Wang, J., 2013. "Fuel suitability for low temperature combustion in compression ignition engines". *Fuel,* ***109***(C), pp. 336–349.

[21] Lacey, J. S., Filipi, Z. S., Sathasivam, S. R., Cannella, W. J., and Fuentes-Afflick, P. A., 2013. "HCCI Operability Limits: The Impact of Refinery Stream Gasoline Property Variation". *J. Eng. Gas. Turb. Power,* ***135***(8), p. 081505.

[22] Rapp, V. H., Cannella, W. J., Chen, J.-Y., and Dibble, R. W., 2013. "Predicting Fuel Performance for Future HCCI Engines". *Combust. Sci. Technol.,* ***185***(5), pp. 735–748.

[23] Zhao, H., Li, J., Ma, T., and Ladommatos, N., 2002. Performance and analysis of a 4-stroke multi-cylinder gasoline engine with CAI combustion. SAE Technical Paper 2002-01-0420.

[24] Curran, S. J., Cho, K., Briggs, T. E., and Wagner, R. M., 2011. "Drive cycle efficiency and emissions estimates for reactivity controlled compression ignition in a multi-cylinder light-duty diesel engine". In ASME 2011 Internal Combustion Engine Division Fall Technical Conference (ICEF2011), no. ICEF2011-60227, pp. 557–564.

[25] Kenney, T., Gardner, T. P., Low, S. S., Eckstrom, J. C., Wolf, L. R., Korn, S. J., and Szymkowicz, P. G., 2001. Overall results: Phase I ad hoc diesel fuel test program. SAE Technical Paper 2001-01-0151.

[26] Szymkowicz, P. G., French, D. T., and Crellin, C. C., 2001. Effects of advanced fuels on the particulate and NO_x emissions from an optimized light-duty CIDI engine. SAE Technical Paper 2001-01-0148.

[27] Gao, Z., Daw, C. S., Wagner, R. M., Edwards, K. D., and Smith, D. E., 2012. "Simulating the impact of premixed charge compression ignition on light-duty diesel fuel economy and emissions of particulates and NO_x". *Proc. IMechE. Part D: J. Automobile Engineering,* ***227***(1), pp. 31–51.

[28] Gao, Z., Daw, C. S., and Wagner, R. M., 2012. "Simulating study of premixed charge compression ignition on light-duty diesel fuel economy and emissions control". In Spring Technical Meeting of the Central States Section of the Combustion Institute.

[29] Ortiz-Soto, E., Assanis, D. N., and Babajimopoulos, A., 2012. "A comprehensive engine to drive-cycle modelling framework for the fuel economy assessment of advanced engine and combustion technologies". *Int. J. Engine Res.,* ***13***(3), pp. 287–304.

[30] Ahn, K., Whitefoot, J., Babajimopoulos, A., Ortiz-Soto, E., and Papalambros, P. Y., 2012. "Homogeneous charge compression ignition technology implemented in a hybrid electric vehicle: System optimal design and benefit analysis for a power-split architecture". *Proc. IMechE. Part D: J. Automobile Engineering,* ***227***(1), pp. 87–98.

[31] EPA Office of Transportation and Air Quality, 2013. Dynamometer drive schedules. http://www.epa.gov/nvfel/testing/dynamometer.htm.

[32] Wipke, K. B., Cuddy, M. R., and Burch, S. D., 1999. "ADVISOR 2.1: A user-friendly advanced powertrain simulation using a combined backward/forward approach". *IEEE Trans. Vehicular Technol.,* ***48***(6), pp. 1751–1761.

[33] Markel, T., Brooker, A., Hendricks, T., and Johnson, V., 2002. "ADVISOR: a systems analysis tool for advanced vehicle modeling". *J. Power Sources,* ***110***(2), pp. 255–266.

[34] Gao, D. W., Mi, C., and Emadi, A., 2007. "Modeling and simulation of electric and hybrid vehicles". *Proc. IEEE,*

95(4), pp. 729–745.

[35] Reilly, D., Andersen, R., Casparian, R., and Dugdale, P., 1991. Saturn DOHC and SOHC four cylinder engines. SAE Technical Paper 910676.

[36] Heywood, J. B., 1988. *Internal Combustion Engine Fundamentals*. McGraw-Hill, New York.

[37] Reaction Design, 2013. *CHEMKIN 10131*. San Diego.

[38] Aldawood, A., Mosbach, S., and Kraft, M., 2012. HCCI combustion control using dual-fuel approach: Experimental and modeling investigations. SAE Technical Paper 2012-01-1117.

[39] Gao, Z., Conklin, J. C., Daw, C. S., and Chakravarthy, V. K., 2010. "A proposed methodology for estimating transient engine-out temperature and emissions from steady-state maps". *Int. J. Engine Res.,* ***11***(2), pp. 137–151.

[40] Nüesch, S., Hellström, E., Jiang, L., and Stefanopoulou, A., 2013. "Influence of transitions between SI and HCCI combustion on driving cycle fuel consumption". In European Control Conference, pp. 1976–1981.

[41] Aceves, S. M., Flowers, D. L., Westbrook, C. K., Smith, J. R., Pitz, W. J., Dibble, R. W., and Christensen, M., 2000. A multi-zone model for prediction of HCCI combustion and emissions. SAE Technical Paper 2000-01-0327.

[42] Fiveland, S. B., and Assanis, D. N., 2001. Development of a two-zone HCCI combustion model accounting for boundary layer effects. SAE Technical Paper 2001-01-1028.

[43] Yelvington, P., and Green, W., 2003. Prediction of the knock limit and viable operating range for a homogeneous-charge compression-ignition (HCCI) engine. SAE Technical Paper 2003-01-1092.

[44] Chin, G., and Chen, J.-Y., 2011. "Modeling of emissions from HCCI engines using a consistent 3-zone model with applications to validation of reduced chemistry". *Proc. Combust. Inst.,* ***33***(2), pp. 3073–3079.

[45] Kodavasal, J., McNenly, M. J., Babajimopoulos, A., Aceves, S. M., Assanis, D. N., Havstad, M. A., and Flowers, D. L., 2013. "An accelerated multi-zone model for engine cycle simulation of homogeneous charge compression ignition combustion". *Int. J. Engine Res.,* ***14***(5), pp. 416–433.

[46] Tsurushima, T., 2009. "A new skeletal PRF kinetic model for HCCI combustion". *Proc. Combust. Inst.,* ***32***(2), pp. 2835–2841.

[47] Curran, H. J., Pitz, W. J., Westbrook, C. K., Callahan, C. V., and Dryer, F. L., 1998. "Oxidation of automotive primary reference fuels at elevated pressures". *Proc. Combust. Inst.,* ***27***, pp. 379–387.

[48] Curran, H. J., Gaffuri, P., Pitz, W. J., and Westbrook, C. K., 2002. "A comprehensive modeling study of iso-octane oxidation". *Combust. Flame,* ***129***(3), pp. 253–280.

Appendix: Sample Pressure Profiles

Figures 5a–5d demonstrate selected pressure profiles for the four fuels considered, at 1200 rpm and various equivalence ratios. Pressure profiles shown include cases of incomplete combustion, successful HCCI combustion, and those past the knock limit. As shown in the figures, the profiles moving upwards correspond to increasing equivalence ratios.

Fuel	ON	% operating points	Index
n-heptane	0	2.95 %	6.86
PRF 20	21.7	2.34 %	5.50
PRF 40	42.5	2.50 %	5.87
PRF 70	72.1	0 %	0.0

Table 1: Octane number, operating point coverage, and HCCI index calculations for various PRFs

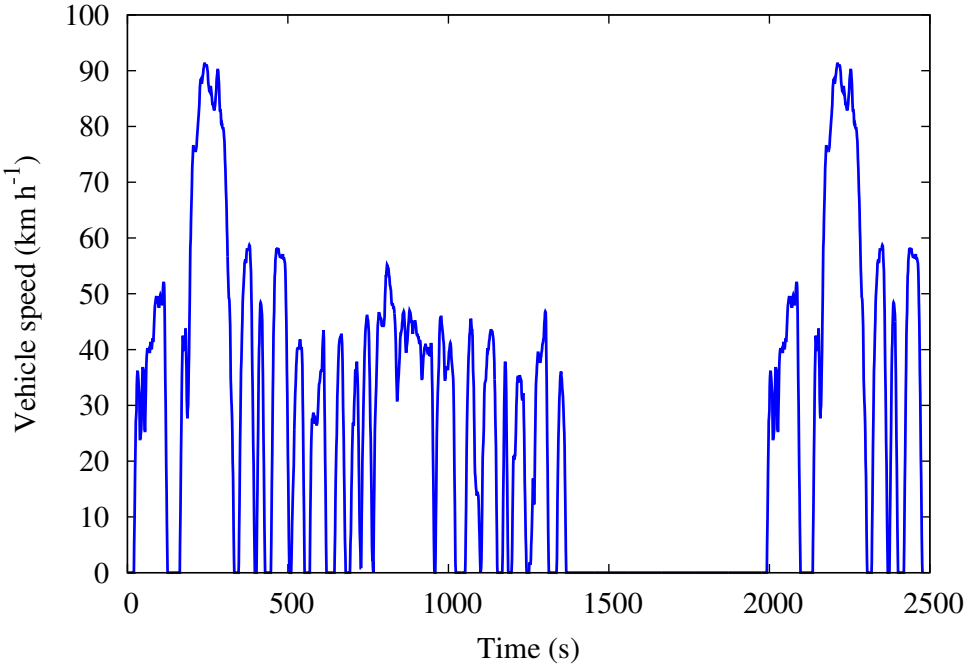

Figure 1: EPA FTP-75 driving cycle

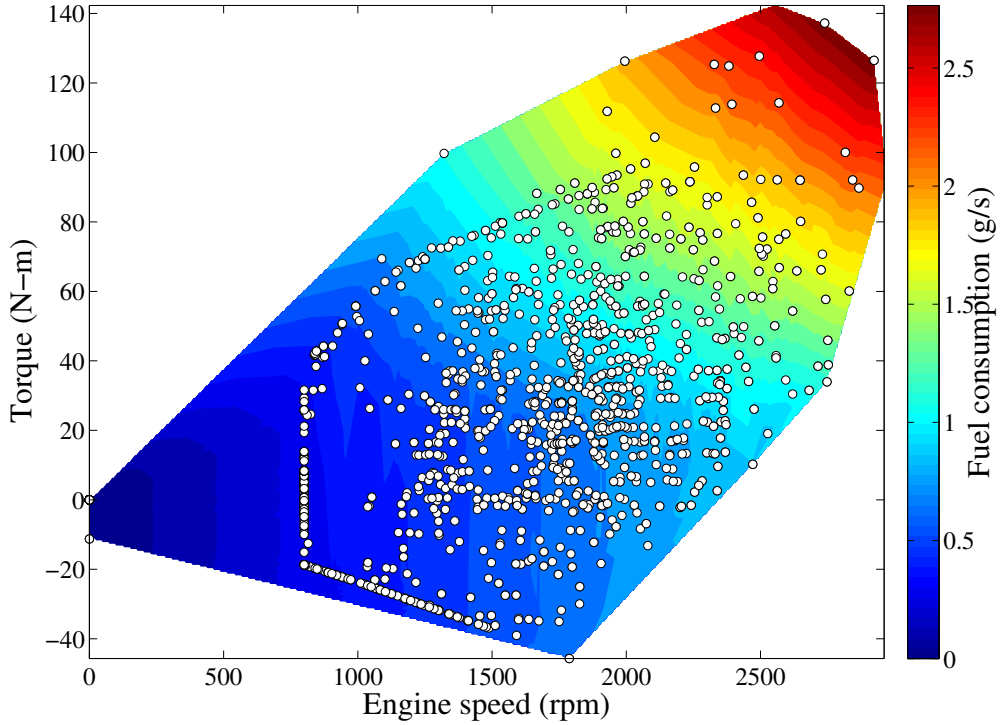

Figure 2: Engine speed and torque operating points with fuel consumption rate overlaid for simulated driving cycle

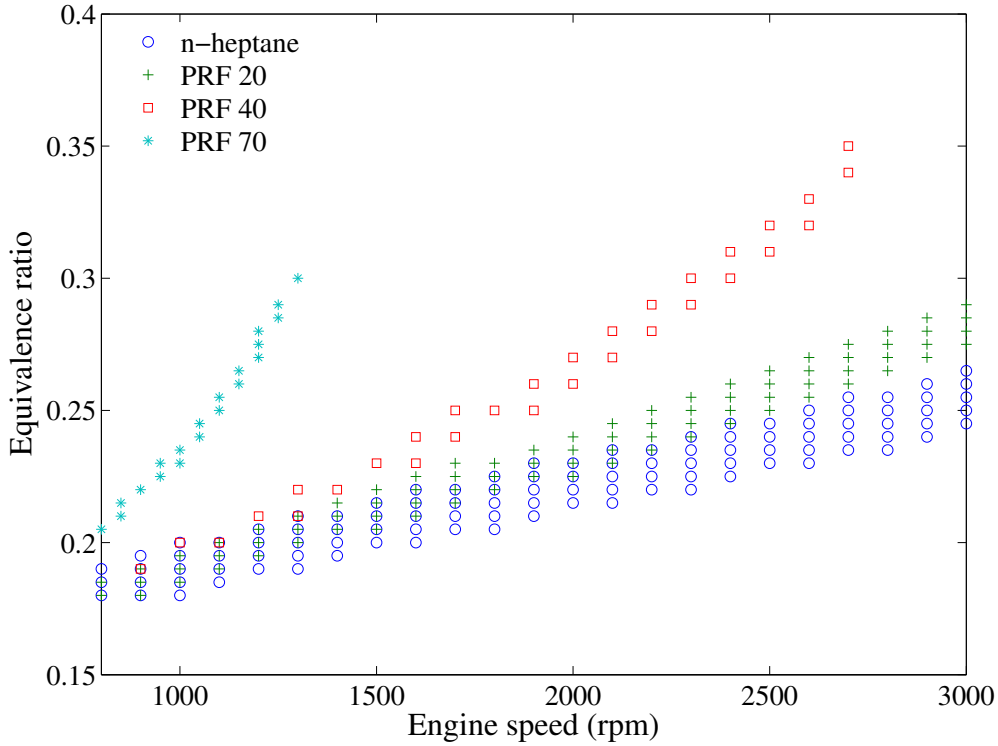

Figure 3: Equivalence ratio operating ranges for various primary reference fuel mixtures at CR = 18 and naturally aspirated inlet conditions

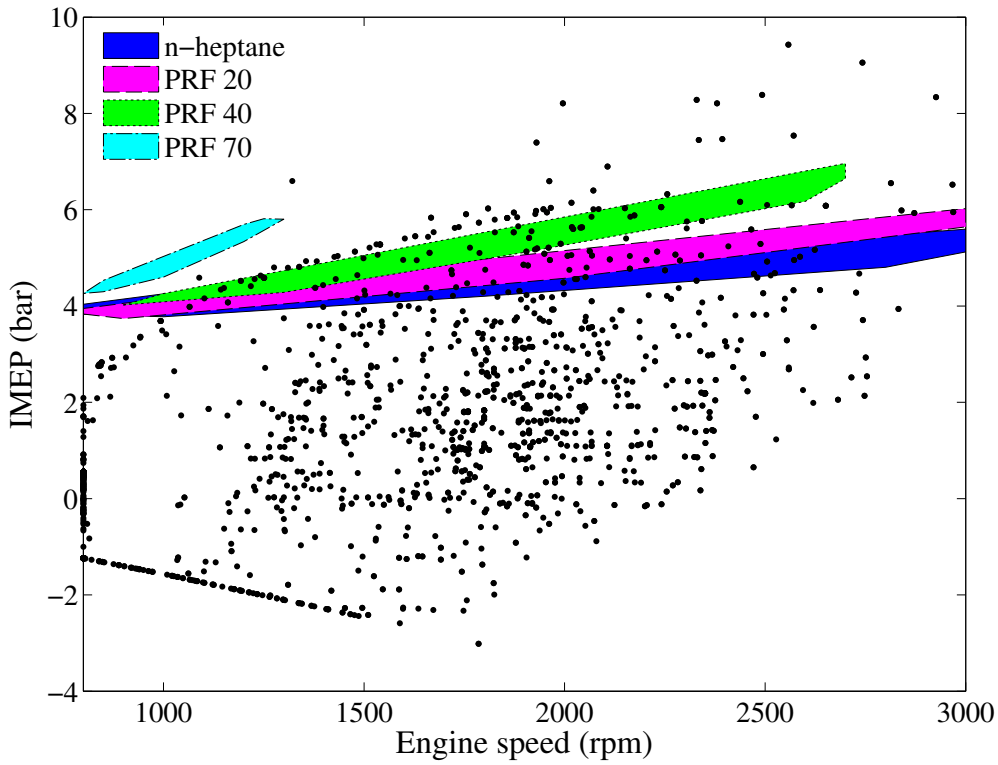

Figure 4: Operating envelopes for various primary reference fuel mixtures at CR = 18 and naturally aspirated inlet conditions over FTP-75 driving cycle

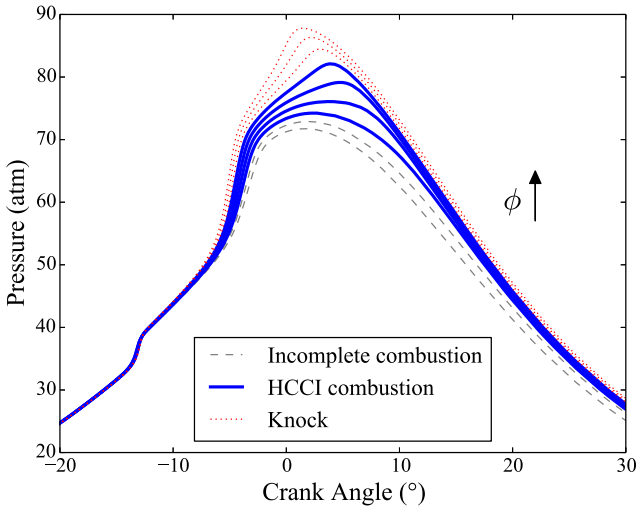

(a) Pressure profiles for PRF 0 (*n*-heptane) at equivalence ratios of 0.18–0.22

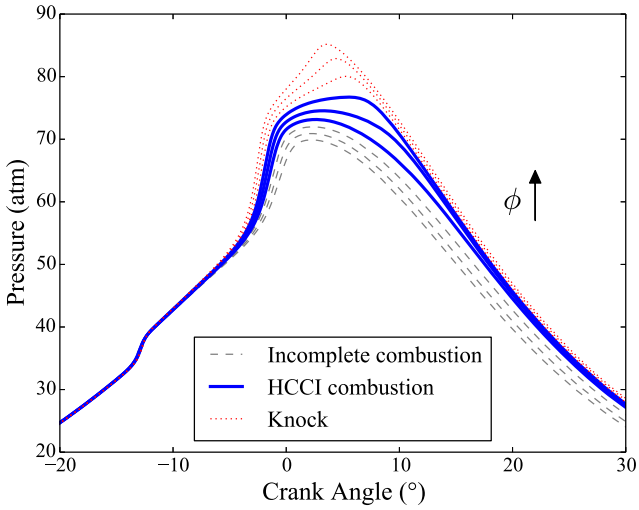

(b) Pressure profiles for PRF 20 at equivalence ratios of 0.18–0.22

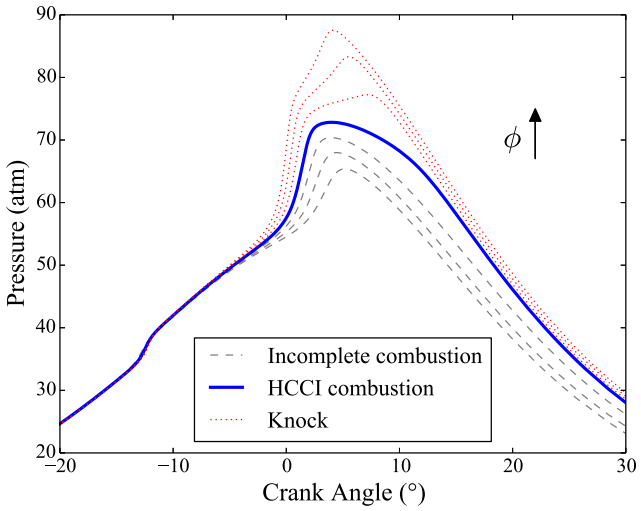

(c) Pressure profiles for PRF 40 at equivalence ratios of 0.18–0.24

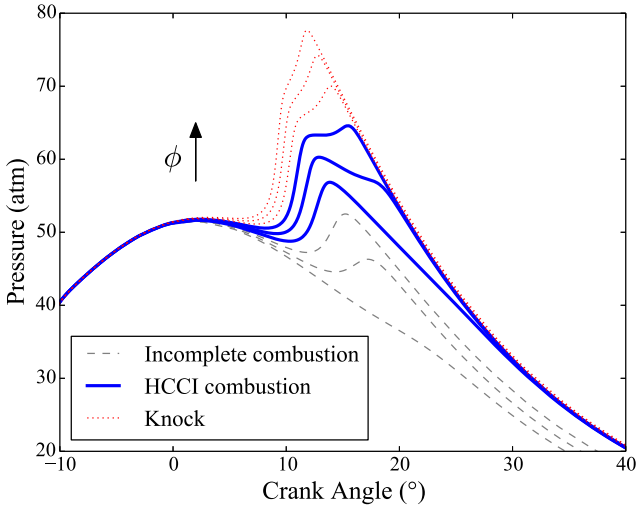

(d) Pressure profiles for PRF 70 at equivalence ratios of 0.265–0.295

Figure 5: Pressure profiles for the fuels at 1200 rpm and various equivalence ratios